Cannabinoid CB$_2$ receptors are involved in the regulation of fibrogenesis during skin wound repair in mice

SHAN-SHAN LI[1,2], LIN-LIN WANG[1], MIN LIU[1], SHU-KUN JIANG[1], MIAO ZHANG[1], ZHI-LING TIAN[1], MENG WANG[1], JIAO-YONG LI[1], RUI ZHAO[1] and DA-WEI GUAN[1]

[1]Department of Forensic Pathology, School of Forensic Medicine, China Medical University, Shenyang, Liaoning 110122; [2]Department of Forensic Medicine, Xuzhou Medical College, Xuzhou, Jiangsu 221002, P.R. China

Abstract. Studies have shown that cannabinoid CB$_2$ receptors are involved in wound repair, however, its physiological roles in fibrogenesis remain to be elucidated. In the present study, the capacity of cannabinoid CB$_2$ receptors in the regulation of skin fibrogenesis during skin wound healing was investigated. To assess the function of cannabinoid CB$_2$ receptors, skin excisional BALB/c mice were treated with either the cannabinoid CB$_2$ receptor selective agonist, GP1a, or antagonist, AM630. Skin fibrosis was assessed by histological analysis and profibrotic cytokines were determined by immunohistochemistry, immunofluorescence staining, reverse transcription-quantitative polymerase chain reaction and immunoblotting in these animals. GP1a decreased collagen deposition, reduced the levels of transforming growth factor (TGF)-β1, TGF-β receptor I (TβRI) and phosphorylated small mothers against decapentaplegic homolog 3 (P-Smad3), but elevated the expression of its inhibitor, Smad7. By contrast, AM630 increased collagen deposition and the expression levels of TGF-β1, TβRI and P-Smad3. These results indicated that cannabinoid CB$_2$ receptors modulate fibrogenesis and the TGF-β/Smad profibrotic signaling pathway during skin wound repair in the mouse.

Introduction

The endocannabinoid system is composed of endogenous ligands, cannabinoid receptors, and synthesizing and degrading enzymes of endogenous ligands. The most extensively investigated cannabinoid receptors are cannabinoid CB$_1$ and cannabinoid CB$_2$ receptors (1). Increasing evidence has demonstrated that cannabinoid CB$_2$ receptor activation decreases fibrosis in mice exhibiting hepatic fibrosis (2), abates skin fibrosis in a mouse model of scleroderma (3), and reduces fibroblast proliferation, and prevents the development of skin and lung fibrosis in a systemic sclerosis mouse model (4). In addition, our previous study demonstrated that cannabinoid CB$_2$ receptors are expressed in a time-dependent manner in neutrophils, macrophages and myofibroblasts during skin wound healing in mice (5). These findings suggest a potential role of cannabinoids in alleviating, or even reversing, skin fibrosis following traumatic damage to the skin.

Wound healing is a dynamically complex but ordered process, which is tightly regulated and comprises an inflammatory stage, a fibrotic stage and a remodeling stage (6). The progress of wound healing requires close interaction between cells and extracellular matrix components, which is controlled through various cytokines, including transforming growth factor (TGF)-α, TGF-β, interleukin-1 and insulin-like growth factor I, (7). Among the multitude of growth factors involved in wound healing, TGF-β has the broadest spectrum of effects (8). TGF-β is closely involved in fibrosis, which appears to markedly enhance the expression levels of matrix components, including fibronectin and collagens (9). Previous evidence has confirmed that cannabinoid CB$_2$ receptor stimulation decreases the expression levels of TGF-β (10) and the downstream mediators, phosphorylated (P)-small mothers against decapentaplegic (Smad)2/3 (3), which suggests that TGF-β is one of the pathways by which cannabinoid CB$_2$ receptors modulates fibrotic events. The present study aimed to investigate the roles of cannabinoid CB$_2$ receptors in the regulation of fibrogenesis and the TGF-β/Smad signaling pathway during skin wound healing in mice.

Materials and methods

Animals and experimental protocol. A total of 155 male, wild-type BALB/c mice (7-9 weeks old; 25±3 g) were housed individually and acclimated to their environment for at least 1 week prior to surgery, in a temperature-controlled animal facility with a 12-h light/dark cycle and *ad libitum* access to water and chow. The present study was approved by the Ethics Committee of China Medical University (Shenyang, China).

Correspondence to: Professor Da-Wei Guan, Department of Forensic Pathology, School of Forensic Medicine, China Medical University, 77 Puhe Road, Shenyang North New Area, Shenyang, Liaoning 110122, P.R. China
E-mail: dwguan@mail.cmu.edu.cn; dwguan@aliyun.com

Experiments conformed to the 'Principles of Laboratory Animal Care' (11), which required minimization of the number of animals included and any suffering that they may experience, and were performed according to the Guidelines for the Care and Use of Laboratory Animals of China Medical University (Shenyang, China).

An animal model of excisional skin wounding was constructed on the basis of previous reports (12-14). Briefly, following intraperitoneal injection with 2% sodium pentobarbital (15 mg/kg; Sigma-Aldrich, St. Louis, MO, USA), two full-thickness circular punch wounds of 6 mm diameter were created symmetrically over the midline of the mouse dorsum. Postoperatively, the mice were housed individually to minimize wound disruption, with access to food and water *ad libitum*.

To evaluate the effects of GP1a and AM630, one group of the injured mice was treated with GP1a, a highly selective cannabinoid CB$_2$ receptor agonist (Ki: 0.037 and 353 nM for cannabinoid CB$_2$ and CB$_1$ receptors, respectively; Tocris Bioscience, Ellisville, MO, USA). A second group was treated with AM630, a cannabinoid CB$_2$ receptor antagonist/inverse agonist (Ki=31.2 nM; Tocris Bioscience), which has 165-fold higher selectivity than the cannabinoid CB$_1$ receptor. GP1a or AM630 was dissolved in dimethylsulfoxide (DMSOU)/Tween-80/physiological saline (5:2:100; all Sigma-Aldrich) at a concentration of 3 mg/kg/day, and was administered by intraperitoneal injection (15-17). Vehicle control mice were injected with 100 μl solvent to determine potential effects of DMSO and Tween-80. Treatment with GP1a or AM630 was started in parallel to excisional challenge and maintained on each subsequent day until the day prior to sacrifice. All mice were sacrificed by intraperitoneal injection with an overdose of sodium pentobarbital. Following sacrifice (12 h and 1, 3, 5, 7, 9, 11, 13, 17 and 21 days post-injury), 1x1 cm specimens were removed from the epicenter of the wound from five mice for each post-traumatic interval. One wound specimen (left or right) was randomly allocated for morphological analyses and the other was allocated for western blot and reverse transcription-quantitative polymerase chain reaction (RT-qPCR) analyses. Five mice without excision were used as a control group.

Tissue preparation and histological analysis. Skin specimens were immediately fixed in 4% paraformaldehyde (Sigma-Aldrich) with phosphate-buffered saline (pH 7.4) and embedded in paraffin. From the specimens, 5 μm-thick sections were obtained and stained using hematoxylin and eosin (HE; Sigma-Aldrich and Perfemiker, Shanghai, China, respectively) and Masson's trichrome staining (Perfemiker), composed of 1 g acid fuchsin, 2 g ponceau and 2 g orange G in 300 ml acetic acid (0.25%). Skin thickness was evaluated under microscopic magnification (x50; cat. no. DM400 B; Leica Microsystems, GmbH, Wetzlar, Germany), by measuring the distance between the epidermis and the dermal-subcuneous fat junction, in five randomly selected fields for each skin section.

Immunohistochemistry and immunofluorescence staining. Skin sections (5 μm) were processed in order to evaluate the expression levels of TGF-β1 (rabbit polyclonal antibody; cat. no. ab92486; Abcam, Cambridge, UK; 1:300 dilution); TGF-β receptor I (TβRI; rabbit polyclonal antibody; cat. no. ab31013; Abcam; 1:3000 dilution); Smad3 ser 423/425 (rabbit polyclonal antibody; cat. no. PAB11304; Abnova; Taipei, China; 1:500 dilution) and Smad7 (rabbit polyclonal antibody; cat. no. ab90085; Abcam; 1:500 dilution). A Histostain-Plus kit (Zymed Laboratories, South San Francisco, CA, USA) was used, according to the manufacturer's protocol. The positive cells were visualized using diaminobenzidine (OriGene Technologies, Beijing, China). Collagen I-positive cells were detected using an immunofluorescence technique by incubating 3 μm skin sections with anti-Collagen I (goat polyclonal antibody; sc-25974; Santa Cruz Biotechnology, Inc., Texas, UT, USA; 1:100 dilution). Hoechst 33258 (cat. no. sc-394039; Santa Cruz Biotechnology, Inc.) was used for nuclei staining. As immunohistochemical controls for the immunostaining procedures, additional sections were incubated with non-immune goat serum or phosphate-buffered saline (pH 7.4) in place of the primary antibodies. Collagen I-positive fibroblast cells (FBCs) were counted independently by two pathologists (magnification, x400) in three sections (five non-contiguous microscope fields for each section) from each lesional skin sample using a Leica DM400 B microscope.

RNA isolation and RT-qPCR. Total RNA was isolated from the skin specimens (100 mg) using RNAiso Plus (cat. no. 9109; Takara Bio, Inc., Shiga, Japan), according to the manufacturer's protocol. Briefly, each skin specimen was cut to 1 mm^3 then treated with 1 ml TRIzol solution (Invitrogen; Thermo Fisher Scientific, Inc., Waltham, MA, USA) for 30 min at room temperature. Following centrifugation at 12,000 x g for 15 min at 4°C, the supernatant was obtained, mixed with chloroform, centrifuged again as before and supplemented with isopropanol (both Perfemiker). Following further centrifugation as before, the precipitate was collected and washed with 75% ethanol (Perfemiker), centrifugation as before, then repeated. The RNA pellet was air-dried and resolved in 60 μl diethylpyrocarbonate-treated dH$_2$O (Takara Bio, Inc.). The optical density value for each RNA sample was measured using a Nanodrop 2000 ultraviolet spectrophotometer (Thermo Fisher Scientific, Inc.). RNA was reverse transcribed into cDNA using a PrimeScript™ RT reagent kit (cat. no. RR037A; Takara Bio, Inc.). RT-qPCR amplification was performed on an ABI 7500 Real-Time PCR system (Applied Biosystems; Thermo Fisher Scientific, Inc.) using a SYBR® PrimeScript™ RT-qPCR kit (cat. no. RR081A; Takara Bio, Inc.). The 20 μl reaction system contained the following: 10 μl SYBR *Premix Ex Taq* (2X), 0.4 μl ROX Dye II, 6 μl dH2O, 0.8 μl PCR forward primer, 0.8 μl PCR reverse primer and 2 μl cDNA. qPCR thermal cycling was performed as follows: One cycle at 95°C for 30 sec, followed by 40 cycles of 95°C for 5 sec and 60°C for 34 sec, and one cycle of 95°C for 15 sec, 60°C for 30 sec and 95°C for 15 sec for fluorescence signal acquisition. Sequence-specific primer pairs were synthesized by Takara Bio, Inc. (Table I). β-actin (Actb) was used as a loading control. Relative quantification was performed using the comparative quantification cycle ($\Delta\Delta$CQ) method. To exclude any potential contamination, negative controls were also included, with dH$_2$O, in place of cDNA, during each run. No amplification product was detected. The RT-qPCR procedure was repeated at least three times for each sample.

Table I. Sequences of the primers used for reverse transcription-quantitative polymerase chain reaction analysis.

Gene	GenBank ID	Primer	Sequence (5'-3')	Product size (bp)
Actb	NM_007393	Forward	ACCTTCTACAATGAGCTGCG	147
		Reverse	CTGGATGGCTACGTACATGG	
Tgfb1	NM_011577	Forward	CCTGAGTGGCTGTCTTTTGA	124
		Reverse	CGTGGAGTTTGTTATCTTTGCTG	
Tgfbr1	NC_000070.6	Forward	ATTGCTCGACGCTGTTCTATTGGT	269
		Reverse	CCTTCCTGTTGGCTGAGTTGTGA	
Smad3	NM_016769	Forward	CCGAGAACACTAACTTCCCTG	84
		Reverse	CATCTTCACTCAGGTAGCCAG	
Smad7	NM_001042660	Forward	GTGTTGCTGTGAATCTTACGG	118
		Reverse	CATTGGGTATCTGGAGTAAGGAG	
Col1a1	NM_007742	Forward	CATAAAGGGTCATCGTGGCT	150
		Reverse	TTGAGTCCGTCTTTGCCAG	
Col3a1	NM_009930	Forward	GAAGTCTCTGAAGCTGATGGG	149
		Reverse	TTGCCTTGCGTGTTTGATATTC	
Acta2	NM_007392	Forward	GTGAAGAGGAAGACAGCACAG	146
		Reverse	GCCCATTCCAACCATTACTCC	

Actb, β-actin; Tgfb, transforming growth factor-β; Smad, small mothers against decapentaplegic; Col1, collagen I; Acta, actin α.

Protein preparation and immunoblotting assay. Skin samples were homogenized in phosphorylated protein lysis buffer (cat. no. KGP9100; KeyGEN Biotech Co., Ltd., Nanjing, China) using a Sonic Ruptor 400 ultrasound (Omni, Inc., Kennesaw, GA, USA) at 4˚C. The homogenates were centrifuged three times at 12,000 x g for 30 min at 4˚C, and the resulting supernatants were collected. Protein concentrations were determined using a Bicinchoninic Acid kit (cat. no. P0010; Beyotime Institute of Biotechnology; Shanghai, China), according to the manufacturer's protocol. Subsequently, 30 μg protein was separated on 12% polyacrylamide gels (Sigma-Aldrich). The protein lysates were then transferred onto polyvinylidene fluoride membranes (EMD Millipore, Billerica, MA, USA) for 100 V for 1 h at room temperature. Membranes were subsequently incubated with 8% skimmed milk for 4 h, washed for a few seconds with Tris-buffered saline containing 0.1% Tween-20 (TBS-T; Perfemiker) and were then incubated with primary antibodies overnight at 4˚C. The specifications and dilutions for the primary antibodies were as follows: Rabbit anti-TGF-β1 polyclonal antibody (cat. no. ab92486; Abcam; 1:400 dilution); rabbit anti-TβRI polyclonal antibody (cat. no. ab31013; Abcam; 1:1,000 dilution); rabbit anti-Smad3 ser 423/425 polyclonal antibody (cat. no. PAB11304; Abnova; 1:10,000 dilution) and rabbit anti-Smad7 polyclonal antibody (cat. no. ab90085; Abcam; 1:500 dilution). Mouse anti-β-actin monoclonal antibody (cat. no. sc-47778; Santa Cruz Biotechnology, Inc; 1:5,000 dilution) was used as a loading control. Following rinsing with TBS-T, the membranes were incubated with polyclonal goat anti-rabbit (cat. no. sc-2054) and anti-mouse (cat. no. sc-2055; both 1:5,000 dilution) secondary antibodies for 90 min at room temperature. Blots were visualized using western blotting luminal reagent (cat. no. sc-2048; all Santa Cruz Biotechnology, Inc.) on an Electrophoresis Gel Imaging Analysis system (cat. no. 5500; Tanon, Shanghai, China). The bands of the blot were quantified by densitometry using ImageJ software (ImageJ 1.48 v; National Institutes of Health, Bethesda, MA, USA).

Statistical analysis. Results are presented as the mean ± standard deviation. One-way analysis of variance was then used to determine the significant differences using SPSS for Windows 13.0 (SPSS, Inc., Chicago, IL, USA). $P<0.05$ was considered to indicate a statistically significant difference.

Results

Effects of GP1a and AM630 on fibrosis. HE staining revealed that, in the vehicle-treated group, numerous polymorphonuclear cells were detected microscopically at 12 h and 1 day post-injury. Mononuclear cells (MNCs), spindle-shaped FBCs and endothelial cells appeared in the wounded zone at 3 days post-injury. Fibrotic tissue formation was observed at 5 days, and became more evident between 9 and 21 days post-injury. The results of the HE and Masson's trichrome staining revealed that the GP1a-treated mice exhibited less collagen deposition and slender fibers, compared with the vehicle-treated mice. By contrast, the mice treated with AM630 exhibited increased collagen deposition and thicker fibers between days 9 and 21 post-injury (Fig. 1A-E).

Skin fibrosis was evaluated by measuring the skin thickness of the wounded area. Between days 9 and 21 post-injury, GP1a-treated group exhibited a considerable decrease in skin thickness, whereas the AM630-treated group exhibited increased skin thickness in the HE-stained sections, compared with the vehicle group (Fig. 1F, $P<0.05$). Collagen I, for the detec-
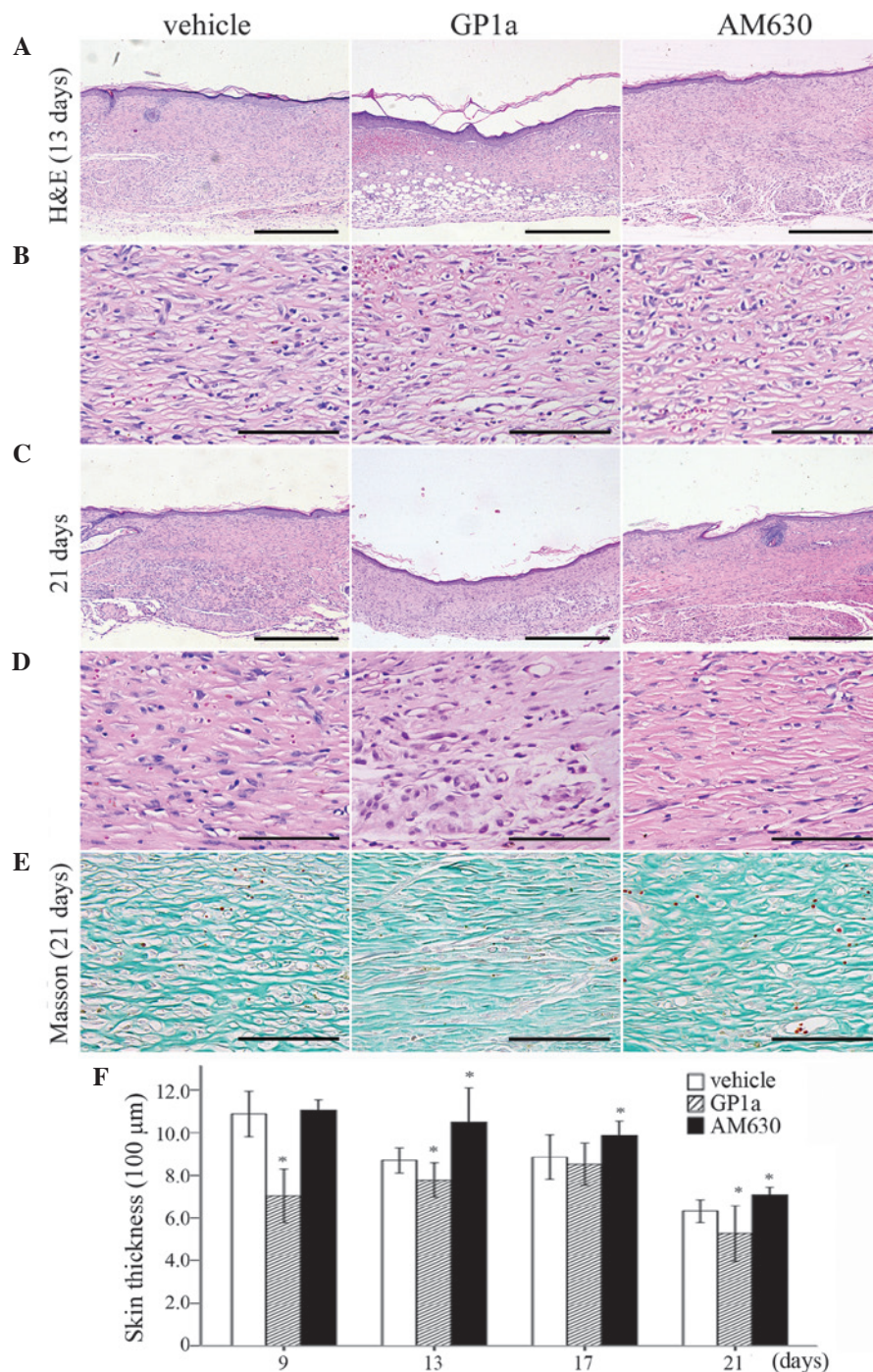
Figure 1. Morphological changes in the fibrosis stage of wound healing. HE staining of the damage zone 13 days post-GP1a or AM630 treatment. Scale bar=(A) 500 μm and (B) 100 μm; HE staining of the damage zone 21 days post-GP1a or AM630 treatment. Scale bar=(C) 500 μm and (D) 100 μm. (E) Masson's trichrome staining of the damage zone at 21 days post-GP1a or AM630 treatment (scale bar=100 μm). (F) Measurements of skin thickness at 9, 13, 17 and 21 days post-GP1a or AM630 treatment. All values are expressed as the mean ± standard deviation (n=5). *P<0.05, compared with the vehicle group. HE, hematoxylin and eosin.

tion of FBCs, was detected using immunofluorescence staining. FBCs began to emerge 5 days post-injury. No significant differences were detected in the number of FBCs among the vehicle, GP1a and AM630 groups at days 5 and 7 post-injury. Following GP1a treatment, there was a decrease in the number of FBCs in the lesional skin, compared with the vehicle group, whereas treatment with AM630 resulted in an increase in the number of FBCs, compared with the vehicle group between days 9 and 21 post-injury (Fig. 2; P<0.05). These findings were consistent

with the results of the RT-qPCR analysis. The mRNA expression levels of Col1a1, Col3a1 and actin α (Acta)2 were marginally elevated at 12 h, peaked for Col3a1 and Acta2 at 7 days, and for Col1a1 at 9 days, and then reduced gradually in the vehicle group. Treatment with GP1a significantly downregulated the mRNA expression levels of Col1a1, Col3a1 and Acta2 in the GP1a-treated group, compared with the vehicle group, whereas AM630 upregulated mRNA expression levels of Col1a1, Col3a1 and Acta2 (Fig. 3; P<0.05).
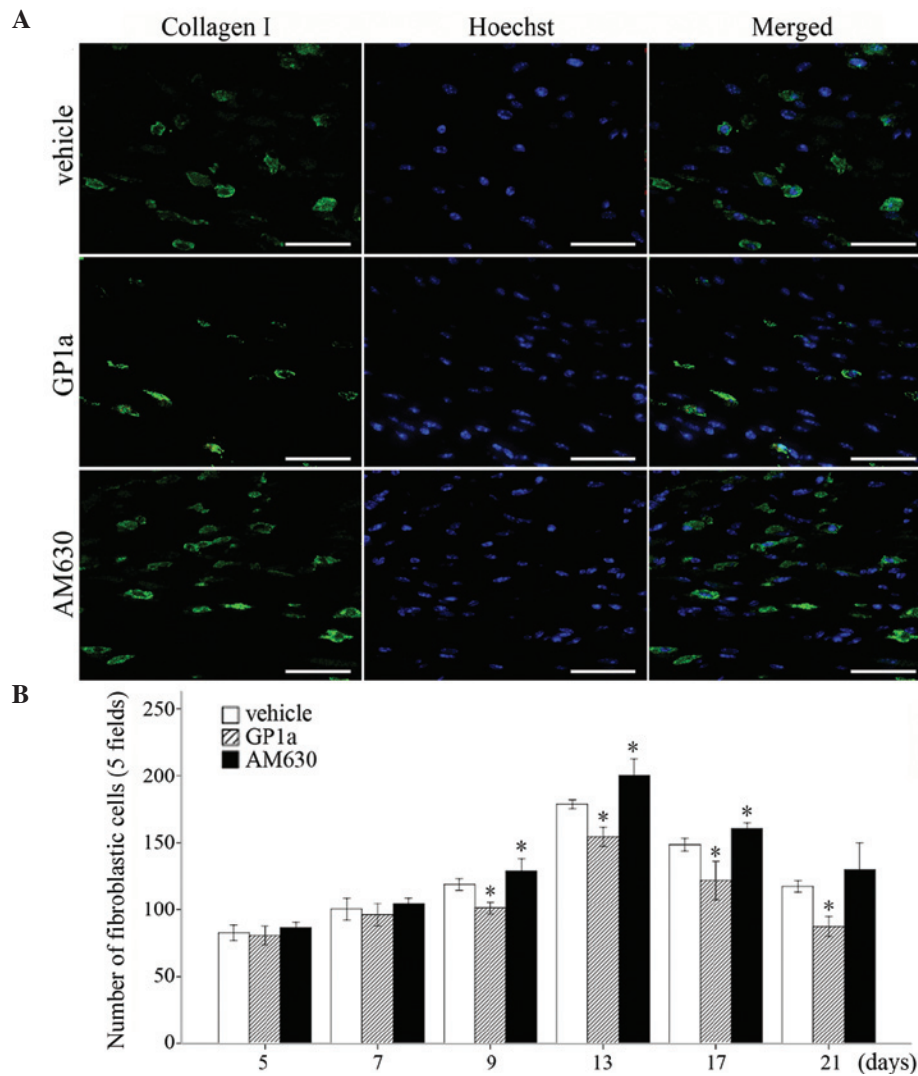
Figure 2. Immunofluorescence analysis was performed to determine the numbers of fibroblast cells. (A) Collagen I immunostaining was present in the wound zone at 13 days post-injury (green color). The nuclei were counterstained with Hoechst 33258 (blue color). Scale bar=50 μm. (B) Histograms showing the numbers of fibroblast cells in five microscopic fields. All values are expressed as the mean ± standard deviation (n=5). *P<0.05, compared with the vehicle group.

Effects of GP1a and AM630 on the TGF-β/Smad signaling pathway. Immunostaining indicated that, in the control skin specimens, positive cytoplasmic immunoreactivities of TGF-β1, TβRI and Smad7 were detected in the epidermis, hair follicles, cutaneous muscle layer and vascular walls, whereas P-Smad3 immunostaining was detected in the nuclei. In the excisional skin samples, no immunostaining for TGF-β1, TβRI, P-Smad3 or Smad7 were observed in polymorphonuclear cells at 12 h or on day 1. Immunoreactivities for TGF-β1, TβRI, P-Smad3 and Smad7 were predominantly observed in the MNCs and FBCs between 3 and 7 days post-injury. Between days 9 and 21 post-wounding, the immunoreactivities were predominantly detected in the FBCs. At 21 days post-injury, the majority of the FBCs exhibited weak immunostaining for TGF-β1, TβRI, P-Smad3 and Smad7 (Fig. 4).

To evaluate the effects of GP1a and AM630 on the TGF-β/Smad signaling, the relative mRNA expression levels of Tgfb1, Tgfbr1, Smad3 and Smad7 in the skin specimens were assayed using RT-qPCR at each of the post-traumatic intervals following excision (Fig. 5). The mRNA expression of Tgfb1 was upregulated markedly within 5 days, and reduced gradually between 7 and 21 days post-injury. The expression of Tgfbr1 increased slowly and reached a peak at 9 days. The mRNA expression of Smad3 was marginally and persistently raised at post-traumatic intervals between 12 h and 21 days, whereas the mRNA expression of Smad7 decreased between 12 h and 5 days, but elevated between 7 and 21 days. The mRNA expression levels of Tgfb1 and Tgfbr1 were downregulated in the GP1a-treated mice, compared with the vehicle-treated mice, whereas the opposite was noted in the mice treated with AM630. In the GP1a group of mice, the mRNA expression of Smad7 was upregulated between 3 and 21 days post-trauma. Significant differences in Smad7 were detected between the AM630 and vehicle group at 3, 5 and 11 days post-traumatic interval. No significant differences were identified among the vehicle, GP1a and AM630 groups for the mRNA expression of Smad3 (Fig. 5).

The results of the western blot analysis of TGF-β1, TβRI, P-Smad3, Smad7 and β-actin for the vehicle-treated samples are shown in Fig. 6A. The relative protein expression levels of TGF-β1 (latent and mature), TβRI, P-Smad3 and Smad7 gradually decreased between 12 h and 3 days, were decreased
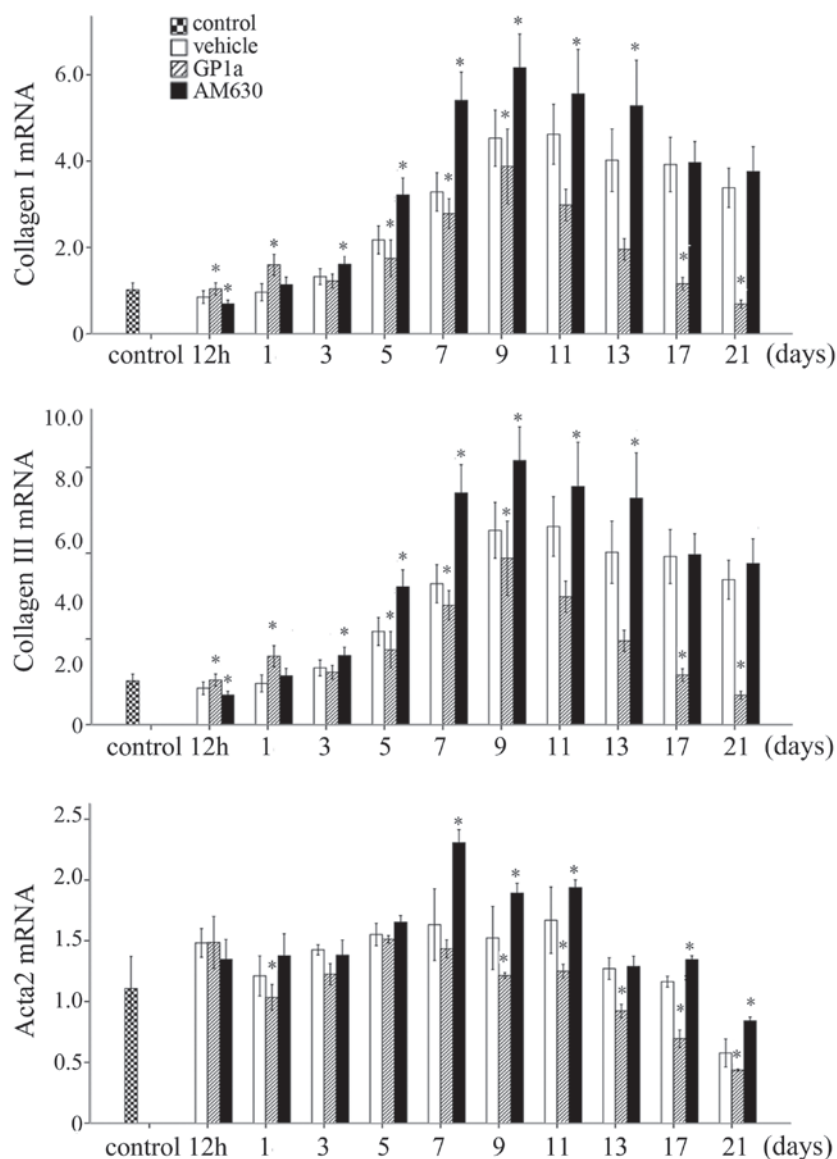
Figure 3. mRNA expression levels of Col1a1, Col3a1 and Acta2 in the vehicle, GP1a- and AM630-treated groups. GP1a decreased the mRNA expression levels of Col1a1, Col3a1 and Acta2, compared with the vehicle group, whereas AM630 increased their expression levels. All values are expressed as the mean ± standard deviation (n=5). *P<0.05, compared with the vehicle group. Col1, collagen I; Acta2, actin α2.

at 5 days post-injury, gradually increased from day 7 and peaked at day 13, prior to decreasing moderately (Fig. 7). The bands of TGF-β1, TβRI, P-Smad3 and Smad7 proteins in the GP1a- and AM630-treated groups are shown in Fig. 6B. Between 12 h and 7 days post-injury, there was a marked upregulation of latent TGF-β1 in the AM630-treated group, however, minimal change was observed in the GP1a group, compared with the vehicle group. From 9 days onwards, the expression of latent TGF-β1 in the GP1a-treated group was substantially lower, compared with that in the vehicle group. In mature TGF-β1, TβRI and P-Smad3, no significant differences were observed among the GP1a, AM630 and vehicle groups between 12 h and 7 days. Between days 9 and 21, the expression levels of mature TGF-β1, TβRI and P-Smad3 in the GP1a group were significantly lower, compared with those in the vehicle group, whereas these levels were increased in the AM630 group. However, the results of Smad7 differed.

Between 12 h and 5 days post-injury, no significant differences were observed among the three groups. Between days 7 and 21 days, Smad7 was markedly increased in the GP1a-treated group, however, minimal change was observed in the AM630-treated group, compared with the vehicle group (Fig. 7; P<0.05).

Discussion

The present study investigated the effects of GP1a and AM630 on excisional wound healing in skin. The data demonstrated that GP1a markedly attenuated fibrogenesis, whereas AM630 enhanced fibrotic events during skin wound healing. In addition, the expression levels of fibrosis-associated genes, Col1a1, Col3a1 and Acta2 were downregulated by GP1a and upregulated by AM630, indicating that cannabinoid CB$_2$ receptors modulated fibrogenesis in mouse skin wound repair.
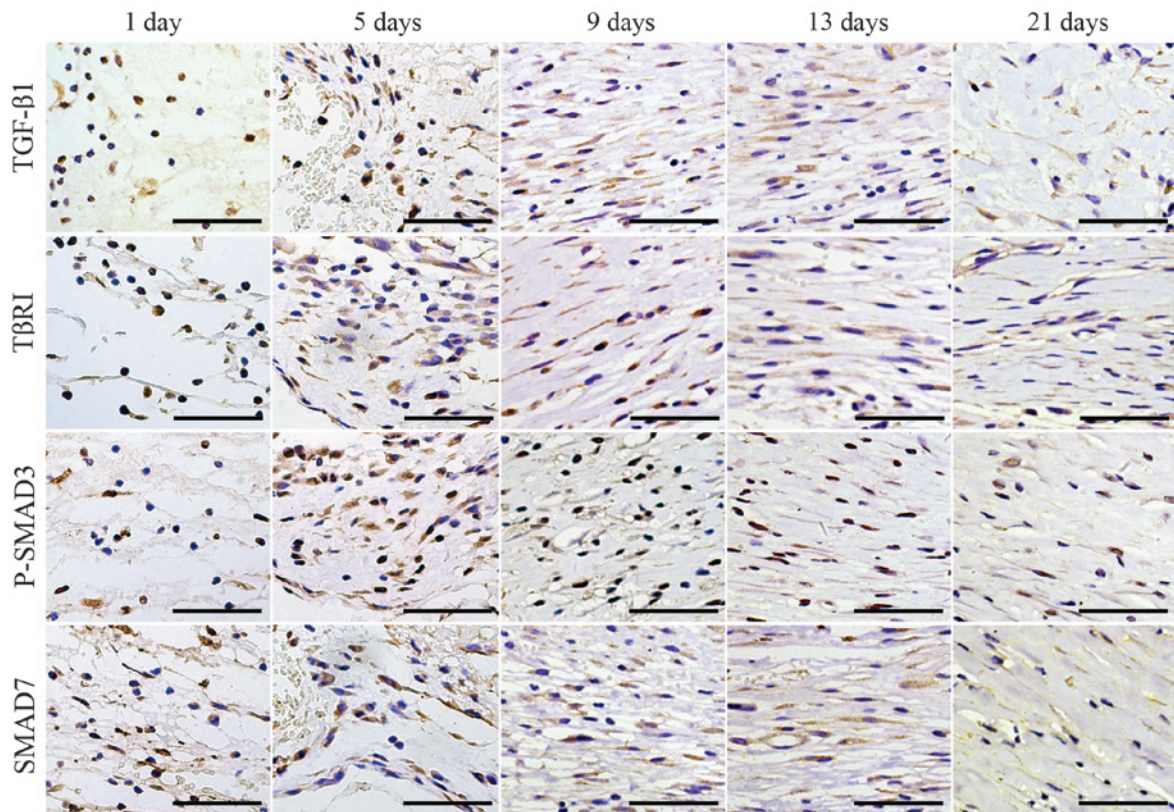
Figure 4. Immunostaining of TGF-β1, TβRI, P-Smad3 and Smad7 at 1, 5, 9, 13 and 21 days post-trauma. In the excisional skin samples, no immunostaining for TGF-β1, TβRI, P-Smad3 or Smad7 were identified in the polymorphonuclear cells at day 1. Immunoreactivities for TGF-β1, TβRI, P-Smad3 and Smad7 were predominantly observed in the mononuclear cells and fibroblast cells at days 5 post-injury. At days 9 and 13 post-injury, immunoreactivities were predominantly detected in the fibroblast cells. Scale bar=50 µm. TGF-β1, transforming growth factor-β1; TβRI, TGF-β receptor type 1; Smad, small mothers against decapentaplegic; P-Smad, phosphorylated Smad.
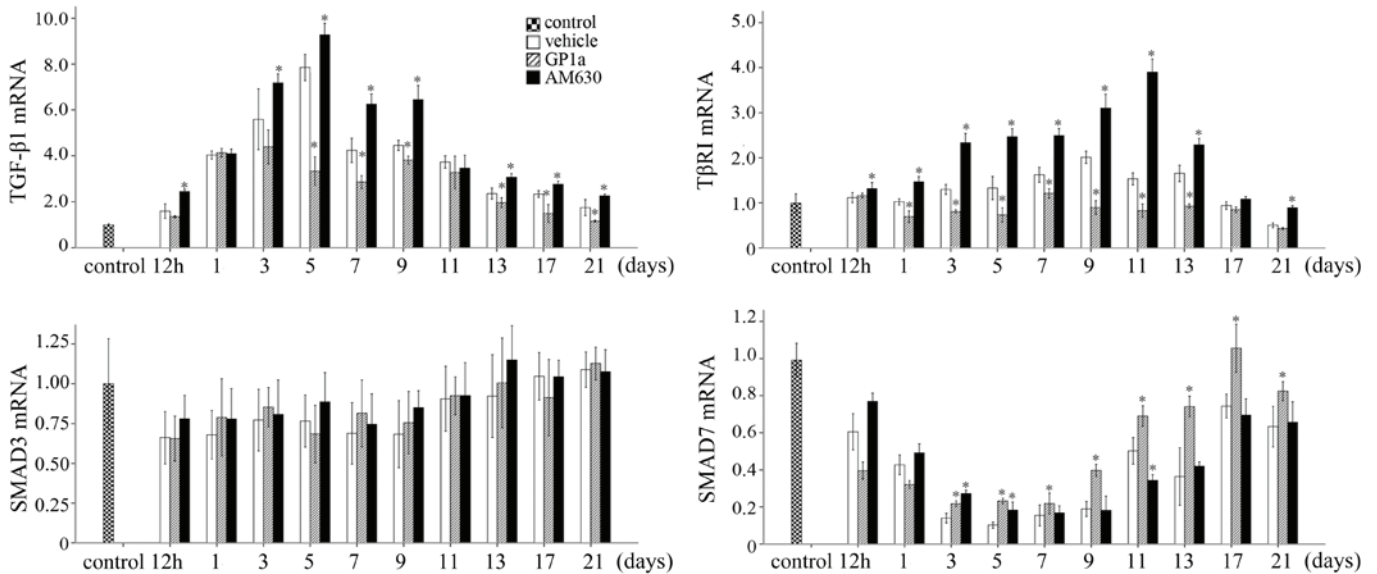
Figure 5. mRNA expression levels of Tgfb1, Tgfbr1, Smad3 and Smad7 in the vehicle, GP1a and AM630 groups. All values are expressed as the mean ± standard deviation (n=5). *P<0.05, compared with the vehicle group. Tgfb1, transforming growth factor-β1; Tgfbr1, TGF-β receptor type 1; Smad, small mothers against decapentaplegic.

Our previous study showed that cannabinoid CB$_2$ receptors are detected in the epidermis, hair follicles, sebaceous glands, cutaneous muscle layer and vascular smooth muscle cells in the skin of mice, and are dynamically expressed in neutro-phils, macrophages and myofibroblasts during skin wound healing in mice (5). The primary physiological function of the cutaneous endocannabinoid system is to constitutively control balanced proliferation, differentiation and survival, as well as
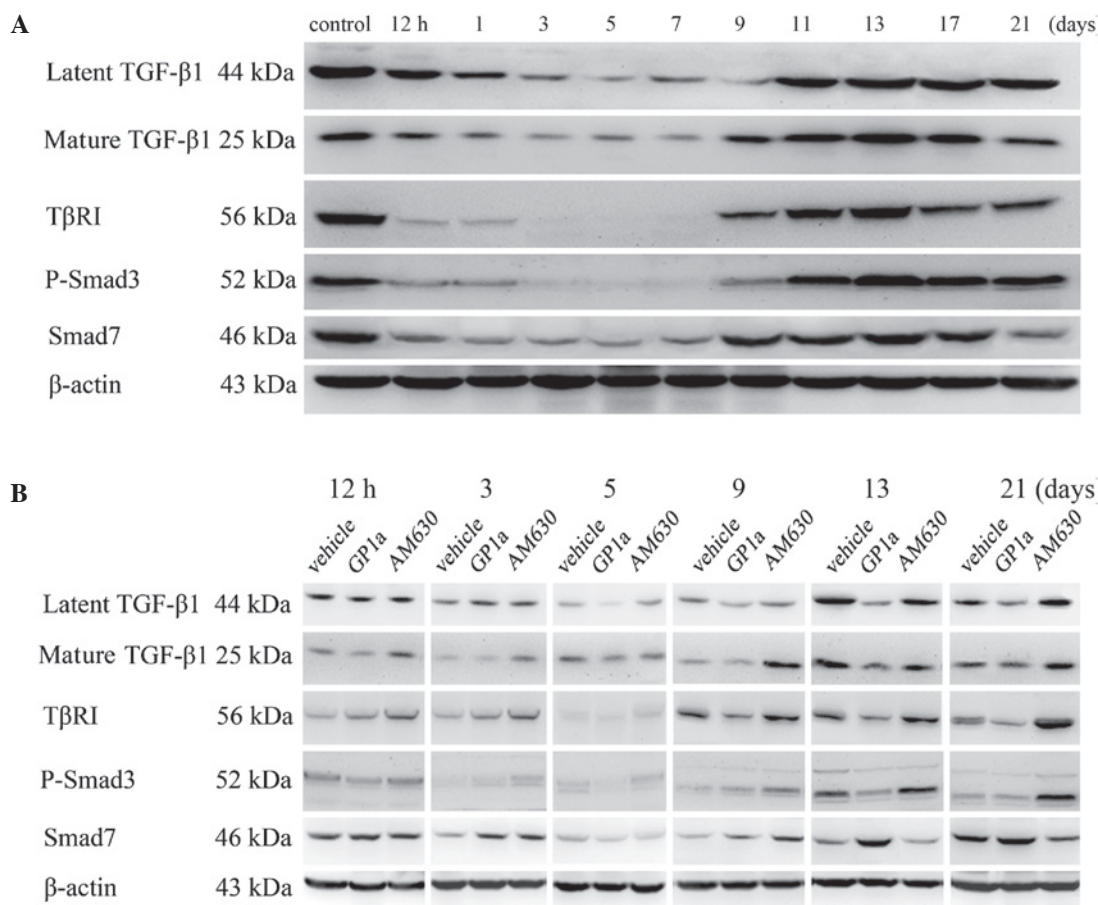
Figure 6. (A) Representative western blots of TGF-β1 (latent and mature), TβRI, P-Smad3 and Smad7 proteins in the vehicle-treated group. (B) Representative western blots of TGF-β1 (latent and mature), TβRI, P-Smad3 and Smad7 proteins in the vehicle-, GP1a- and AM630-treated groups. TGF-β1, transforming growth factor-β1; TβRI, TGF-β receptor type 1; Smad, small mothers against decapentaplegic; P-Smad, phosphorylated Smad.

immune competence and/or tolerance of the skin cells (18). Previous studies have shown that long-term cannabinoid CB₂ receptor stimulation ameliorates cirrhosis in rates subjected to bile duct ligation (19) and the synthetic cannabinoid, WIN55, 212-2 is capable of preventing skin fibrosis in a mouse model of scleroderma (3).

TGF-β is a well-studied fibrotic cytokine and originates from injured epidermis, blood and exudate. Platelets are considered to be the primary source of activated TGF-β immediately following injury (20). Previous studies have demonstrated that cannabinoid CB₂ receptor activation attenuates the expression of TGF-β in hepatic fibrosis (21), myocardial fibrosis (22), subarachnoid hemorrhage (23) and skeletal muscle contusion (24), and disrupts dermal fibrogenesis in a model of bleomycin-induced scleroderma by promoting downregulation of the TGF-β signaling pathway (3). The role of TGF-β in wound healing has been well characterized. Targeting the TGF-β signaling pathway using therapeutic agents to improve wound healing and/or reduce scarring has been successful in pre-clinical investigations (25).

In the present study, TGF-β1 and TβRI were decreased in the GP1a-treated group, but increased in the AM630-treated group, indicating that cannabinoid CB₂ receptors are important in modulating the TGF-β signaling pathway. Smad proteins are the downstream mediators of canonical TGF-β

signaling. The protein level of P-Smad3 was decreased in the GP1a-treated group but increased in the AM630-treated group. However, no significant difference was detected in the mRNA expression of Smad3 between the post-traumatic intervals. These findings suggested that neither GP1a or AM630 modulated the expression of Smad3 at the gene level. As the Smad7 protein is induced by P-Smad3 but inhibits TGF-β signaling by binding to activated TβRI and preventing Smad3 phosphorylation (26), the increased level of Smad7 in fibrosis following treatment with GP1a indicated the inhibition of TGF-β1/Smad3 signaling by negative feedback. Although significant differences were detected between the mRNA expression levels of Smad7 on 3, 5 and 11 days post-traumatic interval, no significant differences in Smad7 protein expression were detected. Taken together, these data suggested that cannabinoid CB₂ receptors exerted a regulatory effect on the TGF-β/Smad signaling pathway, although the role of the endocannabinoid system in fibrogenesis remains to be fully elucidated.

The results of the present study indicated that cannabinoid CB₂ receptors modulate fibrogenesis and the TGF-β/Smad profibrotic signaling pathway during skin wound repair in mice. These findings may improve current understanding of the molecular mechanisms involved in the action of cannabinoid CB₂ receptors in skin wound healing, and offer a potential therapeutic strategy.
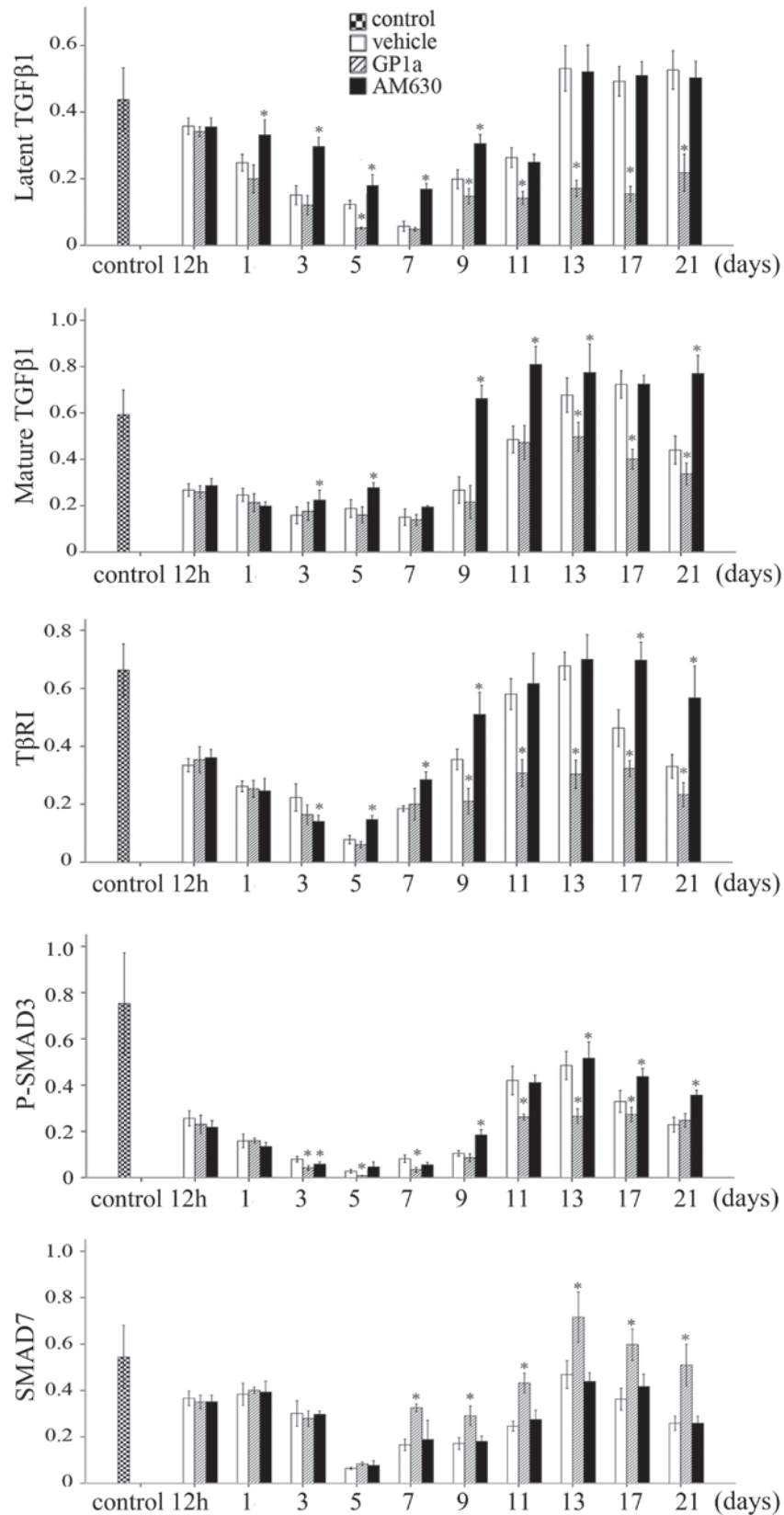
Figure 7. Quantitative analysis of TGF-β1 (latent and mature), TβRI, P-Smad3 and Smad7 proteins following treatment with vehicle, GP1a or AM630. Values are expressed as the mean ± standard deviation (n=5). *P<0.05, compared with the vehicle group. TGF-β1, transforming growth factor-β1; TβRI, TGF-β receptor type 1; Smad, small mothers against decapentaplegic; P-Smad, phosphorylated Smad.

References

1. Mackie K: Cannabinoid receptors: Where they are and what they do. J Neuroendocrinol 20 (Suppl 1): S10-S14, 2008.
2. Guillot A, Hamdaoui N, Bizy A, Zoltani K, Souktani R, Zafrani ES, Mallat A, Lotersztajn S and Lafdil F: Cannabinoid receptor 2 counteracts interleukin-17-induced immune and fibrogenic responses in mouse liver. Hepatology 59: 296-306, 2014.
3. Balistreri E, Garcia-Gonzalez E, Selvi E, Akhmetshina A, Palumbo K, Lorenzini S, Maggio R, Lucattelli M, Galeazzi M and Distler JW: The cannabinoid WIN55, 212-2 abrogates dermal fibrosis in scleroderma bleomycin model. Ann Rheum Dis 70: 695-699, 2011.
4. Servettaz A, Kavian N, Nicco C, Deveaux V, Chéreau C, Wang A, Zimmer A, Lotersztajn S, Weill B and Batteux F: Targeting the cannabinoid pathway limits the development of fibrosis and autoimmunity in a mouse model of systemic sclerosis. Am J Pathol 177: 187-196, 2010.
5. Zheng JL, Yu TS, Li XN, Fan YY, Ma WX, Du Y, Zhao R and Guan DW: Cannabinoid receptor type 2 is time-dependently expressed during skin wound healing in mice. Int J Legal Med 126: 807-814, 2012.
6. Artlett CM: Inflammasomes in wound healing and fibrosis. J Pathol 229: 157-167, 2013.
7. Singer AJ and Clark RA: Cutaneous wound healing. N Engl J Med 341: 738-746, 1999.
8. Finnson KW, Arany PR and Philip A: Transforming growth factor beta signaling in cutaneous wound healing: Lessons learned from animal studies. Adv Wound Care (New Rochelle) 2: 225-237, 2013.
9. Branton MH and Kopp JB: TGF-beta and fibrosis. Microbes Infect 1: 1349-1365, 1999.
10. Zarruk JG, Fernández-López D, García-Yébenes I, García-G utiérrez MS, Vivancos J, Nombela F, Torres M, Burguete MC, Manzanares J, Lizasoain I and Moro MA: Cannabinoid type 2 receptor activation downregulates stroke-induced classic and alternative brain macrophage/microglial activation concomitant to neuroprotection. Stroke 43: 1211-219, 2012.
11. US Office of Science and Technology Policy: Laboratory animal welfare; U.S. government principles for the utilization and care of vertebrate animals used in testing, research and training; notice. Fed Regist 50: 20864-20865, 1995.
12. Wang X, Ge J, Tredget EE and Wu Y: The mouse excisional wound splinting model, including applications for stem cell transplantation. Nat Protoc 8: 302-309, 2013.
13. Galiano RD, Michaels J V, Dobryansky M, Levine JP and Gurtner GC: Quantitative and reproducible murine model of excisional wound healing. Wound Repair Regen 12: 485-492, 2004.
14. Ansell DM, Campbell L, Thomason HA, Brass A and Hardman MJ: A statistical analysis of murine incisional and excisional acute wound models. Wound Repair Regen 22: 281-287, 2014.
15. Guabiraba R1, Russo RC, Coelho AM, Ferreira MA, Lopes GA, Gomes AK, Andrade SP, Barcelos LS and Teixeira MM: Blockade of cannabinoid receptors reduces inflammation, leukocyte accumulation and neovascularization in a model of sponge-induced inflammatory angiogenesis. Inflamm Res 62: 811-821, 2013.
16. Del Fabbro L, Borges Filho C, Cattelan Souza L, Savegnago L, Alves D, Henrique Schneider P, de Salles HD and Jesse CR: Effects of Se-phenyl thiazolidine-4-carboselenoate on mechanical and thermal hyperalgesia in brachial plexus avulsion in mice: Mediation by cannabinoid CB1 and CB2 receptors. Brain Res 1475: 31-36, 2012.
17. Gorantla S, Makarov E, Roy D, Finke-Dwyer J, Murrin LC, Gendelman HE and Poluektova L: Immunoregulation of a CB2 receptor agonist in a murine model of neuroAIDS. J Neuroimmune Pharmacol 5: 456-468, 2010.
18. Bíró T, Tóth BI, Haskó G, Paus R and Pacher P: The endo-cannabinoid system of the skin in health and disease: Novel perspectives and therapeutic opportunities. Trends Pharmacol Sci 30: 411-420, 2009.
19. Mahmoud MF, Swefy SE, Hasan RA and Ibrahim A: Role of cannabinoid receptors in hepatic fibrosis and apoptosis associated with bile duct ligation in rats. Eur J Pharmacol 742: 118-124, 2014.
20. Brunner G and Blakytny R: Extracellular regulation of TGF-beta activity in wound repair: Growth factor latency as a sensor mechanism for injury. Thromb Haemost 92: 253-261, 2004.
21. Lee TY, Lee KC and Chang HH: Modulation of the cannabinoid receptors by andrographolide attenuates hepatic apoptosis following bile duct ligation in rats with fibrosis. Apoptosis 15: 904-914, 2010.
22. Defer N, Wan J, Souktani R, Escoubet B, Perier M, Caramelle P, Manin S, Deveaux V, Bourin MC, Zimmer A, *et al*: The cannabinoid receptor type 2 promotes cardiac myocyte and fibroblast survival and protects against ischemia/reperfusion-induced cardiomyopathy. FASEB J 23: 2120-2130, 2009.
23. Fujii M, Sherchan P, Krafft PR, Rolland WB, Soejima Y and Zhang JH: Cannabinoid type 2 receptor stimulation attenuates brain edema by reducing cerebral leukocyte infiltration following subarachnoid hemorrhage in rats. J Neurol Sci 342: 101-106, 2014.
24. Yu T, Wang X, Zhao R, Zheng J, Li L, Ma W, Zhang S and Guan D: Beneficial effects of cannabinoid receptor type 2 (CB2R) in injured skeletal muscle post-contusion. Histol Histopathol 30: 737-749, 2015.
25. Finnson KW, McLean S, Di Guglielmo GM and Philip A: Dynamics of transforming growth factor beta signaling in wound healing and scarring. Adv Wound Care (New Rochelle) 2: 195-214, 2013.
26. Yan X and Chen YG: Smad7: Not only a regulator, but also a cross-talk mediator of TGF-β signalling. Biochem J 434: 1-10, 2011.